Progress In Electromagnetics Research, PIER 76, 427–447, 2007

EFFECT OF MUTUAL COUPLING AND CONFIGURATION OF CONCENTRIC CIRCULAR ARRAY ANTENNA ON THE SIGNAL-TO-INTERFERENCE PERFORMANCE IN CDMA SYSTEMS

R. Fallahi

Iran Telecommunication Research Center (ITRC)
P. O. Box: 14155-3961, Tehran 1439955471, Iran

M. Roshandel

Mobile Communication of Iran (MCI)
Tehran 1991954651, Iran

Abstract—The suitable use of an array antenna at the base station of a wireless communication system can result in improvement in signal-to-interference ratio (SIR). In the present work, we consider circular array (CA) and concentric circular antenna array (CCAA) that are used for smart antenna systems. The performance criteria for SIR improvement is employed in this paper, is the spatial interference suppression coefficient. We first develop the expression of this figure of merit for CCAA and then analyze and compare the SIR performance for various configurations of eight and nine elements of CA and CCAA, with and without the element in the center by using circular patch antenna are provided. In addition, the effect of mutual coupling (MC) is taken into account.

1. INTRODUCTION

Spatial filtering methods using advanced antenna techniques, smart or adaptive antennas, have received much attention over the last few years [1, 2]. Filtering in the spatial domain can separate spectrally and temporally overlapping signals from multiple mobile users, and hence the performance of system can be significantly improved. Particular

interest in such adaptive antennas has been shown with regard to code-division multiple-access (CDMA) systems. This is because the third-generation cellular networks, e.g., cdma2000 in North America and wide-band CDMA in Europe and Japan, are based on CDMA.

In CDMA systems, all users communicate simultaneously in the same frequency band, and hence multiple-access interference (MAI) is one of the major causes of transmission impairment. The interference rejection or signal-to-interference ratio (SIR) improvement capability is, therefore, an important measure of performance for an array antenna at base station of CDMA-based cellular system. This discrimination ability is in general a function of the array geometry (for example, linear or circular), the number of antenna elements (including their spacing), and the direction of signal arrival of the desired user and the interferers. It is defined as reciprocal of the spatial interference suppression coefficient, which is determined as an average cross-correlation between the beamforming weight vector toward for desired user and the array steering vector toward the interferer [3]. The subject of interference suppression in general from a radar point of view was analyzed in [4]. In the context of CDMA systems, many research papers have addressed the SIR improvement in passing only, while also neglecting MC between antenna elements [3, 5–7]. The applications of the spatial interference suppression coefficient have cropped up in number of recent papers and are mainly concerned with finding the mean value, e.g., in [8], where it is employed in determining an expression for the theoretical bit error rate of smart antenna system, and in [9], where it is used to find the capacity of multi antenna system for CDMA.

In real arrays, MC is always present, and hence it is important to assess the SIR performance when MC is included in the array analysis [10, 11]. A common assumption in the study of MC is that it will lead to degradation in the performance of the system, e.g., it was found in [11] that SIR performance of linear half-wavelength dipole array antenna is degraded by considering MC. But this is not the case in general, on the other hand MC may have positive effect on the SIR performance, e.g., it was found in [11] that SIR performance of circular half-wavelength dipole array antenna is improved by considering MC.

Antenna arrays may be linear, two-dimensional, circular and spherical in element arrangement. A very popular type of antenna arrays is the circular array (CA) which has several advantages over other schemes such as all-azimuth scan capability (i.e., it can perform 360° scan around its center) and the beam pattern can be kept invariant. CCAA that contains many concentric circular rings of different radii and number of elements have several advantages

including the flexibility in array pattern synthesis and design both in narrowband and broadband beamforming applications [12–19]. CCAA is also favored in direction of arrival (DOA) applications since it provides almost invariant azimuth angle coverage.

In this paper, we provide a detailed presentation of the SIR improvement of CA and CCAA by using circular patch antenna. In particular, we consider the effect of array configuration and the center element on the SIR improvement capability. In addition, the effect of MC on the SIR performance is observed. The method of analysis for a patch antenna is method-of-moments (MoM) in a MC environment by using integrated full-wave electromagnetic simulation (IE3D) software [20]. The elements are designed to cover both 1.85 and 2 GHz. These ranges of frequencies are very desirable in CDMA systems.

The remainder of the paper is organized as follows. Section 2 states design of the desire patch antenna for CDMA system. The derivation of the spatial interference suppression coefficient for CA and CCAA by considering MC effect is provided in Section 3. Following these considerations, analysis and comparison of the SIR performance of CA and CCAA are presented in Section 4. Finally, the conclusions of this work are presented in Section 5.

2. CIRCULAR PATCH ANTENNA DESIGN FOR WIRELESS COMMUNICATIONS

In this section, a circular patch antenna for wireless communications is characterized in detail. Now we consider design formulas of the circular patch antenna studied in [21] and list the antenna parameters. The antenna geometry is shown in Fig. 1. The antenna parameters are listed below: (in millimeters) $a = 30$, $h = 1.27$, $(X_f, Y_f) = (7.3, 0)$. Where "a" is radius of the antenna, "h" is the substrate thickness in mm and the dielectric constant is: $\varepsilon_r = 2.33$. Subsequently, the antenna is fed by a coaxial probe and the feed location is (X_f, Y_f). The S_{11} is calculated by IE3D software and measured on an HP-8510 network analyzer. Some experimental results prove the validity of this design. Subsequently, is designed to cover both 1.85 and 2 GHz. These ranges of frequencies are very desirable in modern wireless communications.

3. THEORY

The arrangement of elements in the CCAA may contain multiple concentric circular rings which differ in radii and number of elements

and this gives arise to different radiation patterns. Fig. 2 shows the configuration of CCAA in which there are M concentric circular rings.

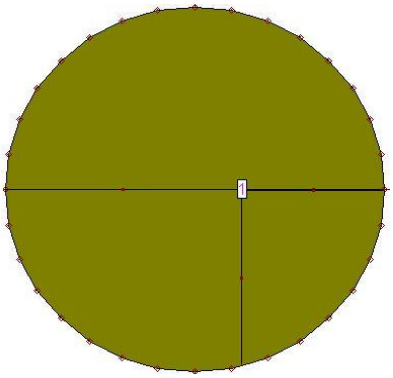

Figure 1. Array element.

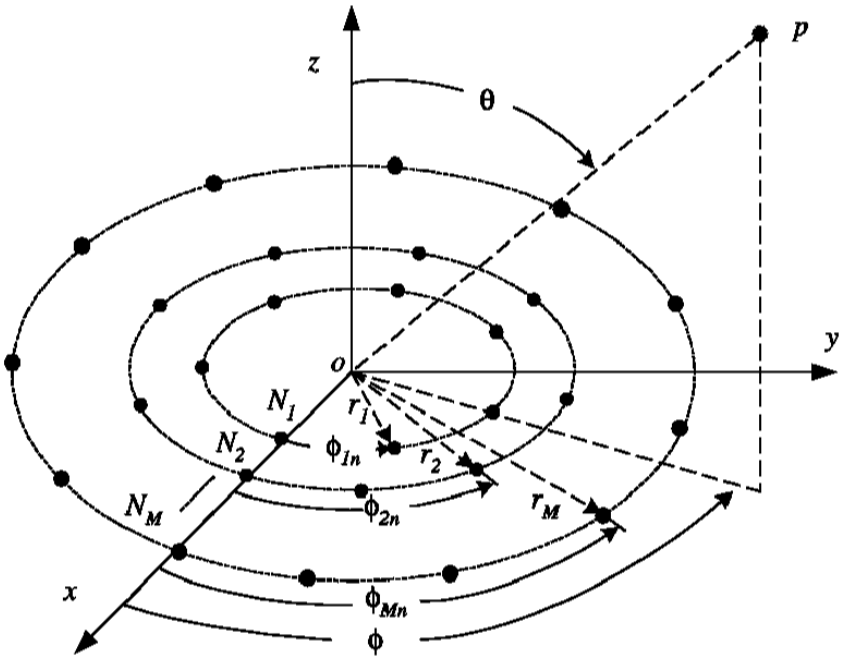

Figure 2. Concentric circular antenna arrays (CCAA).

3.1. Geometry and Array Steering Vector of UCCAA

The mth ring has a radius r_m and number of elements N_m where $m = 1, 2, \ldots, M$. Assuming that the elements are uniformly spaced within the ring so it has an element angular separation given by

$$\psi_m = 2\pi/N \tag{1}$$

and the elements in this ring are therefore located with an angle measured from the x-axis given by

$$\phi_{mn} = n\psi_m, \quad n = 1, 2, \ldots, N_m \tag{2}$$

An expression for the array steering vector can be deduced by first defining the array steering vector for a single ring and extending the analysis for the whole array. For the mth ring, the array steering vector has elements given by

$$a_{mn}(\theta, \phi) = e^{j\kappa r_m \sin(\theta)\cos(\phi - \phi_{mn})} \tag{3}$$

where κ is the wave number $= 2\pi/\lambda$, $\lambda =$ wavelength of the carrier frequency of the signals, therefore the array steering vector for such ring will be:

$$\begin{aligned}\mathbf{a}_m(\theta, \phi) \;=\; & \left[e^{j\kappa r_m \sin(\theta)\cos(\phi - \phi_{m1})} \quad e^{j\kappa r_m \sin(\theta)\cos(\phi - \phi_{m2})}\right. \\ & \left. \ldots e^{j\kappa r_m \sin(\theta)\cos(\phi - \phi_{mn})} \ldots e^{j\kappa r_m \sin(\theta)\cos(\phi - \phi_{mN_m})}\right]^T\end{aligned} \tag{4}$$

Now, the array steering vector for the whole array can be formulated as:

$$\mathbf{a}(\theta, \phi) = [\mathbf{a}_1(\theta, \phi)\mathbf{a}_2(\theta, \phi) \ldots \mathbf{a}_m(\theta, \phi) \ldots \mathbf{a}_M(\theta, \phi)]^T \tag{5}$$

Generally, rings may have different number of elements, thus array steering vectors of rings have unequal lengths. Array steering vectors of all rings come in one CCAA steering vector. On the other hand, at first the steering vector of the first ring comes then after last element of the first ring, the steering vector of the second ring comes and so on. So, the CCAA steering vector dimensions will be $N \times 1$ $(N = N_1 + N_2 + \ldots + N_M)$. Thus, the CCAA steering vector is:

$$\begin{aligned}\mathbf{a}(\theta, \phi) = & \left[e^{j\kappa r_1 \sin(\theta)\cos(\phi - \phi_{11})} \ldots e^{j\kappa r_1 \sin(\theta)\cos\left(\phi - \phi_{1N_1}\right)}\right. \\ & e^{j\kappa r_2 \sin(\theta)\cos(\phi - \phi_{21})} \ldots e^{j\kappa r_2 \sin(\theta)\cos\left(\phi - \phi_{2N_2}\right)} \\ & \ldots e^{j\kappa r_m \sin(\theta)\cos(\phi - \phi_{m1})} \ldots e^{j\kappa r_m \sin(\theta)\cos(\phi - \phi_{mN_m})} \\ & \left. \ldots e^{j\kappa r_M \sin(\theta)\cos(\phi - \phi_{M1})} \ldots e^{j\kappa r_M \sin(\theta)\cos\left(\phi - \phi_{MN_M}\right)}\right]^T_{N\times 1}\end{aligned} \tag{6}$$

3.2. Signal Model

The array receives signals from K narrow-band mobile users, which are randomly distributed in the xy-plane (azimuthal direction) in the far field of the array and hence, in the above equations $\sin(\theta) = 1$. In this case, the parameter that characterizes the location of the source is its angle of arrival (AOA)ϕ, which is conventionally measured from the x-axis. For simplicity, we first ignore MC and consider the CCAA to be made of omnidirectional antenna elements. For convenience, we select the center of the circle as the phase reference; by considering Equation (3) the received signal at the nth antenna element of the mth ring can be expressed as

$$x_{mn}(t) = \sum_{k=1}^{K} s_k(t) e^{j\kappa r_m \cos(\phi_k - \phi_{mn})} + n_{mn}(t) \tag{7}$$

where $s_k(t) =$ signal transmitted by the kth source as received by the reference antenna, $\phi_k =$ arrival angle of the kth source as measured from the x-axis, and $n_{mn}(t) =$ additive white Gaussian noise at the antenna elements with zero mean and having variance σ^2. Using vector notation, the received signal can be expressed as

$$\mathbf{x}(t) = \sum_{k=1}^{K} \mathbf{a}(\phi_k) \mathrm{s}_k(t) + \mathbf{n}(t) = \mathbf{A}(\phi)\mathbf{s}(t) + \mathbf{n}(t) \tag{8}$$

where $\mathbf{x}(t)$ is an $N \times 1$ vector of measured voltages, $s(t)$ is a $K \times 1$ signal vector, $n(t)$ is an $N \times 1$ noise vector, and $\mathbf{A}(\phi) = [\mathbf{a}(\phi_1), \mathbf{a}(\phi_2), \ldots, \mathbf{a}(\phi_K)]$ is an $N \times K$ matrix whose columns are steering vectors of the sources. The $N \times 1$ steering vector $\mathbf{a}(\phi_k)$ models the spatial response of the array due to an incident plane wave from the ϕ_k direction and is given by

$$\begin{aligned} \mathbf{a}(\phi_k) \;=\; & \Big[e^{j\kappa r_1 \cos(\phi_k - \phi_{11})} \ldots e^{j\kappa r_1 \cos\left(\phi_k - \phi_{1N_1}\right)} \\ & e^{j\kappa r_2 \cos(\phi_k - \phi_{21})} \ldots e^{j\kappa r_2 \cos\left(\phi_k - \phi_{2N_2}\right)} \\ & \ldots e^{j\kappa r_m \cos(\phi_k - \phi_{m1})} \ldots e^{j\kappa r_m \cos(\phi_k - \phi_{mN_m})} \\ & \ldots e^{j\kappa r_M \cos(\phi_k - \phi_{M1})} \ldots e^{j\kappa r_M \cos\left(\phi_k - \phi_{MN_M}\right)} \Big]^T_{N\times 1} \end{aligned} \tag{9}$$

The array correlation matrix associated with vector $\mathbf{x}(t)$ contains information about how signals from each element are correlated with each other and is given by

$$\mathbf{R}_{xx} = \mathbf{E}\left[\mathbf{X}(t)\mathbf{X}^H(t)\right] \tag{10}$$

where $E[.]$ denotes expectation or statistical averaging operator and $(.)^H$ denotes Hermitian transpose.

Let $s_1(t)$ be the desired signal source arriving from direction ϕ_1 and consider the rest of the signals $s_k(t)$, $k = 2, 3, \ldots, K$ as interferences arriving from their respective directions. The array output is given by

$$y(t) = \mathbf{w}^H \mathbf{x}(t) \tag{11}$$

where $\mathbf{w}$ is the weight vector that is applied to the antenna array to produce a beam pattern with its main lobe in the direction of the desired user. Assuming that maximum signal-to-noise ratio beamforming is performed, $\mathbf{w}$ is given by

$$\mathbf{w} = \eta_1 \mathbf{v}_{\max} \tag{12}$$

where $\mathbf{v}_{\max}$ is the eigenvector corresponding to the largest eigenvalue $\lambda_{\max}$ of $\mathbf{R}_{xx}$. It was shown in [22] that the eigenvector corresponding to the maximum eigenvalue of the array correlation matrix is approximately equal to the steering vector of the desired user when the desired signal is much stronger than the interferers at the receiver. Thus $\mathbf{w}$ is given by

$$\mathbf{w} = \eta_1 \mathbf{a}(\phi_1) \tag{13}$$

where η_1 is a constant and is set to $1/N$. Thus the array becomes the phased array as the magnitudes of the weight vector are constant and only the phases are varying. Substituting Equation (13) in Equation (11) and using Equation (8) and simplifying, we get

$$y(t) = s_1(t) + \frac{1}{N} \sum_{k=2}^{K} s_k(t) \mathbf{a}^H(\phi_1) \mathbf{a}(\phi_k) + \frac{1}{N} \mathbf{a}^H(\phi_1) \mathbf{n}(t) \tag{14}$$

The mean output power of the processor is

$$\begin{aligned} P(t) &= E\left[y(t) y^*(t)\right] \\ &= E\left[|s_1(t)|^2\right] + \sum_{k=2}^{K} \frac{1}{N^2} \left|\mathbf{a}^H(\phi_1)\mathbf{a}(\phi_k)\right|^2 E\left[|s_k(t)|^2\right] \\ &\quad + E\left[\frac{1}{N}\left|\mathbf{a}^H(\phi_1)\mathbf{n}(t)\right|^2\right] \\ &= E\left[|s_1(t)|^2\right] + \sum_{k=2}^{K} \alpha_k(\phi_1, \phi_k) E\left[|s_k(t)|^2\right] + \frac{\sigma^2}{N} \end{aligned} \tag{15}$$

The first term on the right side of Equation (15) is the desired signal power, whereas the second and third terms represent interference and noise power, respectively.

3.3. Spatial Interference Suppression Coefficient

The coefficient $\alpha_k(\phi_1, \phi_k) = (1/N^2)\left|\mathbf{a}^H(\phi_1)\mathbf{a}(\phi_k)\right|^2$ in Equation (15) is a measure of how much undesired power is picked up from an interferer. This is due to the fact that the array is unable to form a perfect pencil beam radiation pattern toward the desired signal at $\phi = \phi_1$ so the side lobes pick up interfering signals.

The normalized amount of interference power seen from an interferer k at angle of arrival ϕ_k can be expressed in more general form as a scalar product of beamforming weight vector representing phased antenna elements and the array steering vector representing a plane wave as

$$\alpha_k(\phi_1, \phi_k) = \left|\frac{\mathbf{w}^H\mathbf{a}(\phi_k)}{\|\mathbf{w}^H\|\,\|\mathbf{a}(\phi_k)\|}\right|^2 \tag{16}$$

where $(\|.\|)$ denotes the Euclidean norm of a vector. By considering Equation (13) and simplifying, we get

$$\alpha_k(\phi_1, \phi_k) = \frac{1}{N^2}\left|\mathbf{a}^H(\phi_1)\mathbf{a}(\phi_k)\right|^2 \tag{17}$$

Assuming the interferers are uniformly distributed in the range $[-\pi, \pi]$, the mean value of $\alpha_k(\phi_1, \phi_k)$ is given as

$$G_{avg}(\phi_1) = E\left[\alpha_k(\phi_1, \phi_k)\right] = \frac{1}{2\pi}\int_{-\pi}^{\pi}\alpha_k(\phi_1, \phi_k)d\phi_k \tag{18}$$

where $G_{avg}(\phi_1)$ is the spatial interference suppression coefficient [5].

Using Equation (9), the instantaneous SIR at the array output ($\mathrm{SIR_o}$) can be written as

$$\mathrm{SIR_o} = \frac{E\left[|s_1(t)|^2\right]}{\sum_{k=2}^{K}\alpha_k(\phi_1, \phi_k)E\left[|s_k(t)|^2\right]} \tag{19}$$

We see that the SIR at the array output is a function of ϕ_1, the direction of the desired user. The mean SIR at the array output ($\mathrm{SIR_o}$)

can be written in terms of input SIR ($\mathrm{SIR_{in}}$) as

$$\mathrm{SIR_o} = \frac{\mathrm{SIR_{in}}}{G_{avg}(\phi_1)} \tag{20}$$

The average improvement in SIR (Δ) at the array output is then given as

$$\Delta = 10\log_{10}(\frac{1}{G_{avg}(\phi_1)}) = -10\log_{10}(G_{avg}(\phi_1)) \tag{21}$$

3.4. Mutual Coupling

In order to include effect of MC in CCAA, we insert a MC matrix in the model for the received signal, modifying Equation (8) to

$$\mathbf{x}(t) = \sum_{k=1}^{K} \mathbf{C}\mathbf{a}(\phi_k)s_k(t) + \mathbf{n}(t) = \sum_{k=1}^{K} \mathbf{a}_{MC}(\phi_k)s_k(t) + \mathbf{n}(t) \tag{22}$$

where $\mathbf{a}_{MC}(\phi_k) = \mathbf{C}\ \mathbf{a}(\phi_k)$ is the modified array steering vector. In addition, the beamforming weight vector is modified as

$$\mathbf{w}_{MC} = \frac{1}{N}\mathbf{C}\ \mathbf{a}(\phi_1) \tag{23}$$

The coupling matrix $\mathbf{C}$ of the antenna array employed in the above two equations can be written using the most popular technique to solve for the coefficients of the coupling matrix has been provided by [23].

$$\mathbf{C} = \mathbf{S} + \mathbf{I} \tag{24}$$

where $\mathbf{I}$, $\mathbf{S}$ and $\mathbf{C}$ are the Identity matrix, scattering matrix and MC matrix of array, respectively. In this paper, the $\mathbf{S}$ matrix come from the CCAA using integrated full-wave electromagnetic simulation (IE3D) software which is used of method-of-moments (MoM) calculations.

Once the $\mathbf{C}$ matrix has been obtained, the capability of the array including MC effects is assessed by finding the mean output power of the processor, as before, and identifying the signal, noise, and interference power terms, respectively. It can be shown that with MC matrix taken into account, the normalized amount of interference power seen from an interferer k at angle of arrival ϕ_k is

$$\alpha_k(\phi_1, \phi_k) = \left| \frac{\mathbf{w}_{MC}^{H}\mathbf{a}_{MC}(\phi_k)}{\left\|\mathbf{w}_{MC}^{H}\right\| \left\|\mathbf{a}_{MC}(\phi_k)\right\|} \right|^2 \tag{25}$$

where $\mathbf{w}_{MC}$ is given by Equation (23) and $\mathbf{a}_{MC}(\phi_k)$ by Equation (22), respectively. The numerator in Equation (25) after substituting the values becomes

$$\left|\mathbf{w}_{MC}^{H}\mathbf{a}_{MC}(\phi_k)\right|^2 = \left|\left[\frac{1}{N}\mathbf{C}\ \mathbf{a}(\phi_1)\right]^H [\mathbf{C}\ \mathbf{a}(\phi_k)]\right|^2 = \frac{1}{N^2}\left|\mathbf{a}^H(\phi_1)\mathbf{C}^H\mathbf{C}\ \mathbf{a}(\phi_k)\right|^2 \quad (26)$$

Equation (26) is then substituted in Equation (18) to get the spatial interference suppression coefficient for CCAA, when MC is taken into account.

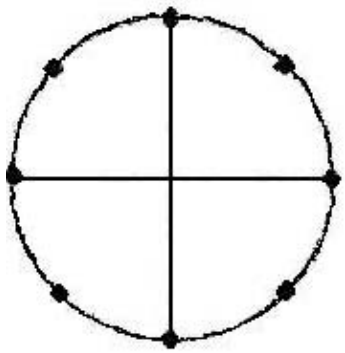

Figure 3. Geometry of "8 elements CA".

4. RESULTS

4.1. 8 Elements CA

The 8 elements circular array is depicted in Fig. 3, hereafter referred to as "8 elements CA". Fig. 4 shows the plot of the spatial interference suppression coefficient $G_{avg}(\theta_1)$ for arrays (a) $r = 0.5\lambda$ and (b) $r = 0.7\lambda$, with and without MC. Under no MC assumption, the SIR improvement of array with smaller radius has a flat curve (see Fig. 4(a)), thus indicates uniform SIR improvement over all angles. But for array with larger radius it has an oscillatory variation (see Fig. 4(b)). When MC is included, $G_{avg}(\theta_1)$ of array with smaller radius indicates MC improves the SIR improvement capability for some scan angles (see Fig. 4(a)). But, $G_{avg}(\theta_1)$ of array with larger

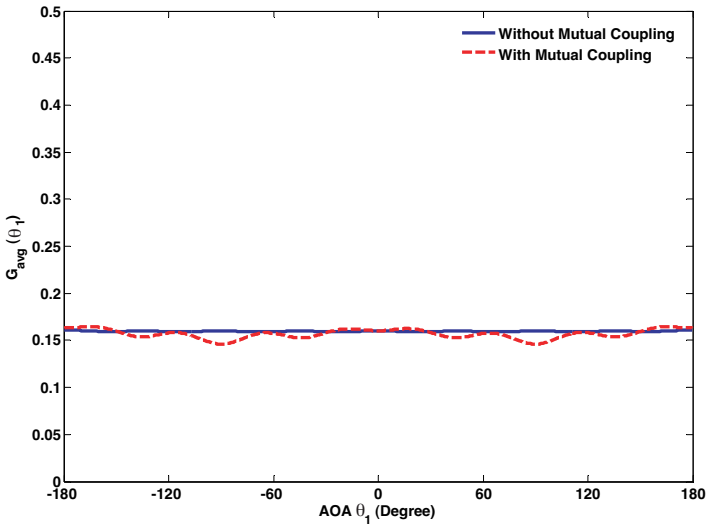

(a)

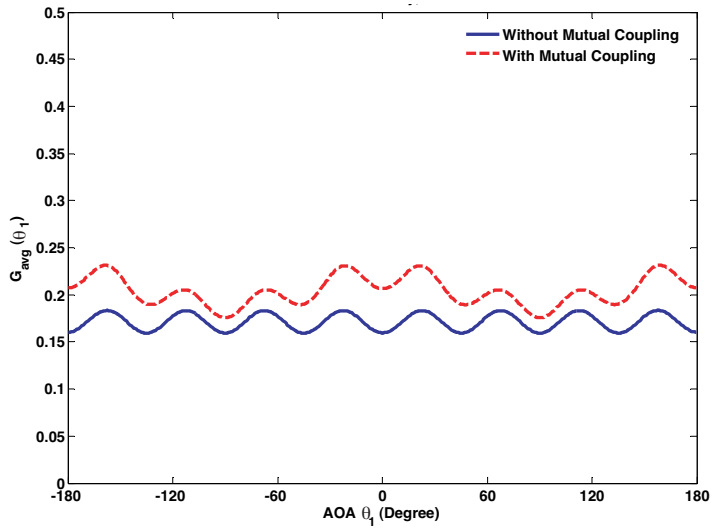

(b)

Figure 4. Variations of $G_{avg}(\theta_1)$ for the "8 elements CA" with different radii, with and without MC; (a) $r = 0.5\lambda$; (b) $r = 0.7\lambda$.

radius indicates it degrades the SIR improvement capability for all (see Fig. 4(b)).

Table 1 shows a comparison of mean of $G_{avg}(\theta_1)$ over θ_1 for arrays, with and without MC. The mean is taken over 360° ($-\pi \leq \theta_1 \leq \pi$). The total average of spatial interference suppression coefficient for the array of $r = 0.5\lambda$ is smaller than array of $r = 0.7\lambda$, when MC is taken into account. Also, it has been shown that pattern characteristics of array with smaller radius are better than array with larger radius [24]. So, from the above results the SIR performance in the array of $r = 0.5\lambda$ is better.

Table 1. Means of $G_{avg}(\theta_1)$ over θ_1 for various configurations of CA and CCAA, with and without MC.

Array		Mean of $G_{avg}(\theta_1)$ over θ_1	
Name	Radius	Without MC	With MC
"8 elements CA"	$r = 0.5\lambda$	0.1596	0.1568
	$r = 0.7\lambda$	0.171	0.2042
"1 + 8 elements CA"	$r = 0.6\lambda$	0.2232	0.2464
	$r = 0.8\lambda$	0.2226	0.1598
"4 + 4 elements CCAA"	$r_1 = 0.45\lambda$, $r_2 = .9\lambda$	0.1934	0.1553
	$r_1 = 0.7\lambda$, $r_2 = \lambda$	0.1599	0.1442
"3 + 5 elements CCAA"	$r_1 = \lambda$, $r_2 = 1.5\lambda$	0.1792	0.2266
"1 + 3 + 4 elements CCAA"	$r_1 = \lambda$, $r_2 = 1.5\lambda$	0.1676	0.2084

4.2. 1 + 8 Elements CA

To investigate the center element effects of circular array on the SIR performance, the 8 elements CA with one element in the center that is referred to as "1 + 8 elements CA" is introduced in Fig. 5. Fig. 6 shows the plot of the spatial interference suppression coefficient $G_{avg}(\theta_1)$ for arrays (a) $r = 0.6\lambda$ and (b) $r = 0.8\lambda$, with and without MC. Under no MC assumption, the SIR improvements of arrays have oscillatory variations. When MC is included, $G_{avg}(\theta_1)$ of array with smaller radius indicates MC degrades the SIR improvement capability for all scan angles, approximately (see Fig. 6(a)). In contrast, $G_{avg}(\theta_1)$ of array with larger radius indicates it improves the SIR improvement capability for all (see Fig. 6(b)).

As is shown in Table 1, the total average of spatial interference suppression coefficient for array of $r = 0.6\lambda$ is larger than array of

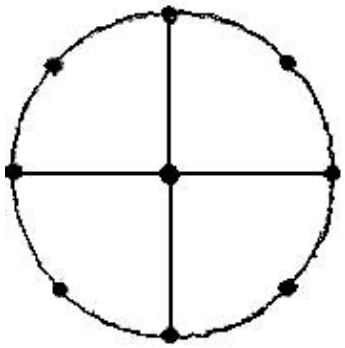

Figure 5. Geometry of "1 + 8 elements CA".

$r = 0.8\lambda$, when MC is taken into account. Also, it has been shown that pattern characteristics of array with larger radius are better than array with smaller radius [24]. Therefore, from the above results we conclude that the SIR performance in array with larger radius is better.

By comparing $G_{avg}(\theta_1)$ of the "1 + 8 elements CA" and the "8 elements CA", we see that, the ripple of the SIR improvement curve in "1 + 8 elements CA" is larger. So, the array performance of "8 elements CA" is more consistent than "1 + 8 elements CA" (has center element).

4.3. 4 + 4 Elements CCAA

In order to improve the SIR performance of CA the CCAA is employed. Two concentric circular arrays that 4 elements are uniformly distributed in the circumference of each ring, hereafter is referred to as "4 + 4 elements CCAA" is introduced in Fig. 7. The included angle of the first element of the second ring connected with the center of circle is β. It's assumed that the radius of inside and outside circles are r_1 and r_2, respectively. The spatial interference suppression coefficient $G_{avg}(\theta_1)$ for arrays (a) $r_1 = 0.7\lambda$, $r_2 = \lambda$, $\beta = 45^\circ$ and (b) $r_1 = 0.45\lambda$, $r_2 = .9\lambda$, $\beta = 45^\circ$, with and without MC are shown in Fig. 8. Because of $\beta = 45^\circ$, these arrays have symmetrical configuration. Under no MC assumption, the SIR improvement of array $r_1 = 0.7\lambda$, $r_2 = \lambda$, $\beta = 45^\circ$, has an oscillatory variation (see Fig. 8(a)). But for array of $r_1 = 0.45\lambda$, $r_2 = .9\lambda$, $\beta = 45^\circ$, it has a flat curve (see Fig. 8(b)), thus, this indicates that the SIR improvement is uniform over all angles. When MC is included, $G_{avg}(\theta_1)$ of array $r_1 = 0.7\lambda$, $r_2 = \lambda$, $\beta = 45^\circ$ indicates MC improves the SIR improvement capability for the most

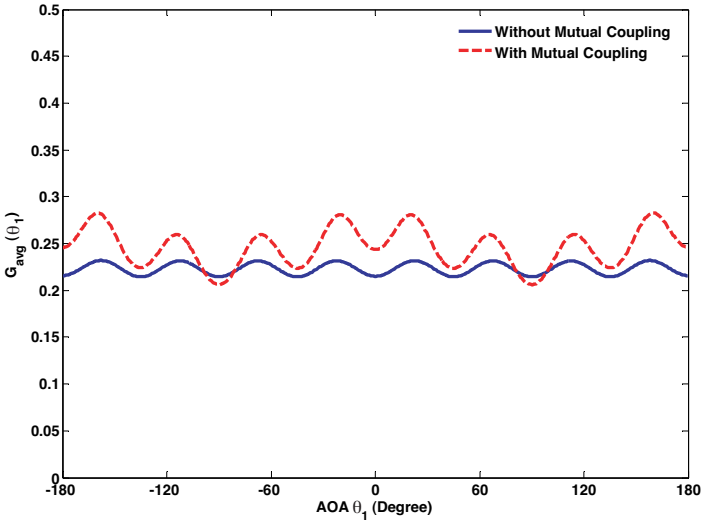

(a)

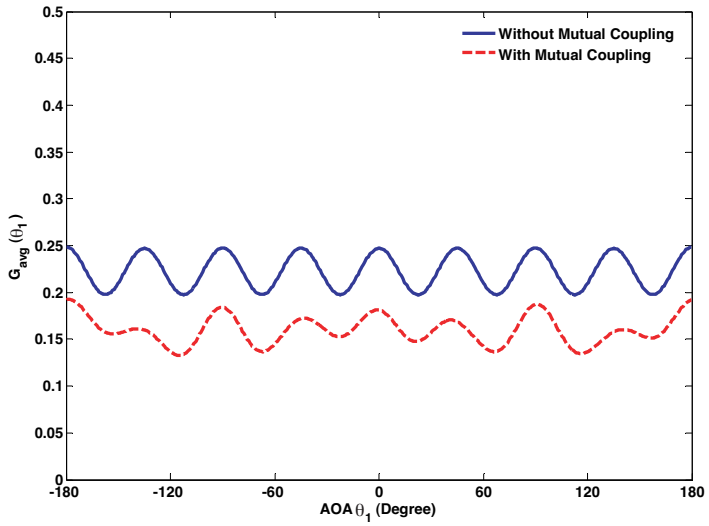

(b)

Figure 6. Variations of $G_{avg}(\theta_1)$ for the "1 + 8 elements CA" with different radii, with and without MC; (a) $r = 0.6\lambda$; (b) $r = 0.8\lambda$.

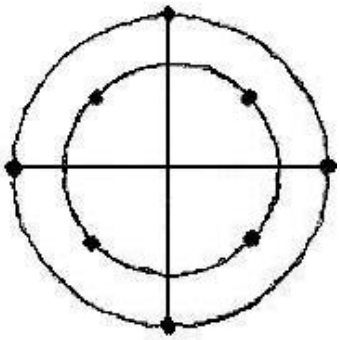

Figure 7. Geometry of "4 + 4 elements CCAA".

scan angles (see Fig. 8(a)). But, $G_{avg}(\theta_1)$ of array $r_1 = 0.45\lambda$, $r_2 = .9\lambda$, $\beta = 45^\circ$ indicates it improves the SIR improvement capability for all (see Fig. 8(b)).

As is shown in Table 1 the total average of spatial interference suppression coefficient for array $r_1 = 0.7\lambda$, $r_2 = \lambda$, $\beta = 45^\circ$ is smaller than array $r_1 = 0.45\lambda$, $r_2 = .9\lambda$, $\beta = 45^\circ$, when MC is taken into account. Also, it has been shown that pattern characteristics in array $r_1 = 0.7\lambda$, $r_2 = \lambda$, $\beta = 45^\circ$, are better than array $r_1 = 0.45\lambda$, $r_2 = .9\lambda$, $\beta = 45^\circ$ [24]. In despite of above results, the array performance of array $r_1 = 0.45\lambda$, $r_2 = .9\lambda$, $\beta = 45^\circ$, is more consistent than array $r_1 = 0.7\lambda$, $r_2 = \lambda$, $\beta = 45^\circ$, because of the flatten curve.

4.4. 3 + 5 Elements CCAA

In this section we investigate the effect of asymmetric configuration of the CCAA on the SIR performance. The inner and outer circles have three and five elements, respectively, hereafter is referred to as "3 + 5 elements CCAA" is introduced in Fig. 9(a). The plot of the spatial interference suppression coefficient $G_{avg}(\theta_1)$ for array $r_1 = \lambda$, $r_2 = 1.5\lambda$, with and without MC is shown in Fig. 9(b). Under no MC assumption, the SIR improvement has an oscillatory variation (see Fig. 9(b)). When MC is included, $G_{avg}(\theta_1)$ of array indicates MC degrades the SIR improvement capability for the most scan angles (see Fig. 9(b)). By comparing the result of this and "4 + 4 elements CCAA" (symmetrical geometry), we conclude that the ripple of the $G_{avg}(\theta_1)$ in "3 + 5 elements CCAA" is noticeable.

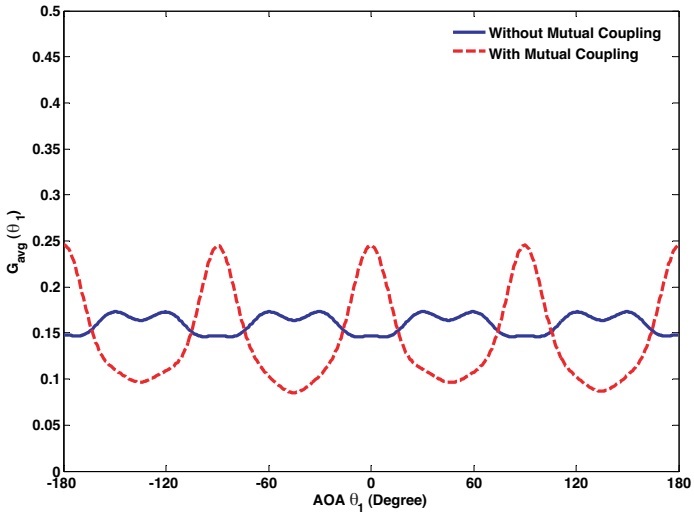

(a)

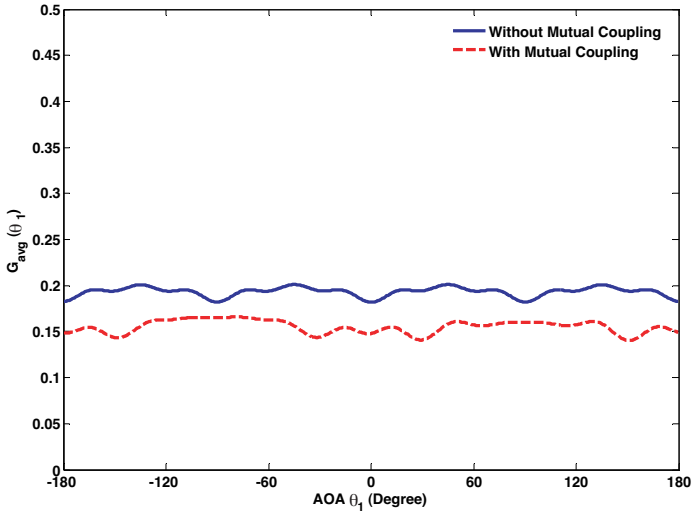

(b)

Figure 8. Variations of $G_{avg}(\theta_1)$ for the "4 + 4 elements CCAA" with different radii, with and without MC; (a) $r_1 = 0.7\lambda$, $r_2 = \lambda$, $\beta = 45°$; (b) $r_1 = 0.45\lambda$, $r_2 = .9\lambda$, $\beta = 45°$.

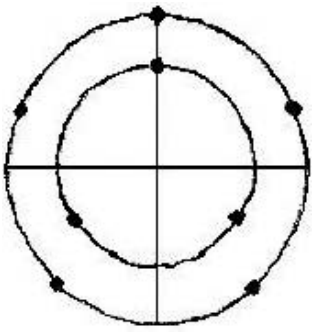

(a)

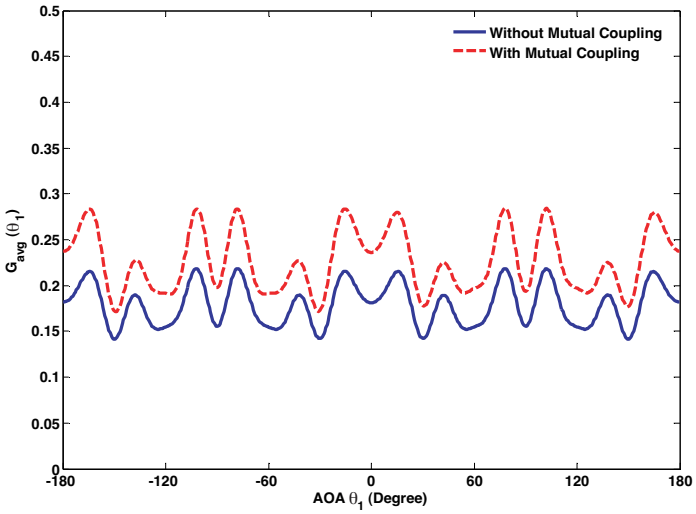

(b)

Figure 9. (a) Geometry of "3 + 5 elements CCAA"; (b) Variations of $G_{avg}(\theta_1)$ for "3 + 5 elements CCAA", with and without MC; with $r_1 = \lambda$, $r_2 = 1.5\lambda$.

4.5. 1 + 3 + 4 Elements CCAA

To investigate the effect of the center element in CCAA, on the SIR performance, "1 + 3 + 4 elements CCAA" is used as shown in Fig. 10(a). The inner and outer circles have three and four elements, respectively and there is one element in the center. The plot of the spatial interference suppression coefficient $G_{avg}(\theta_1)$ for array $r_1 = \lambda$,

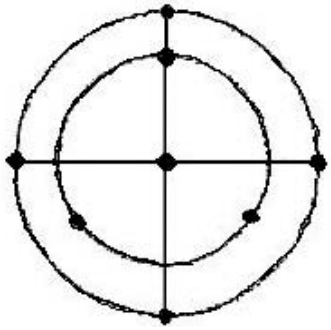

(a)

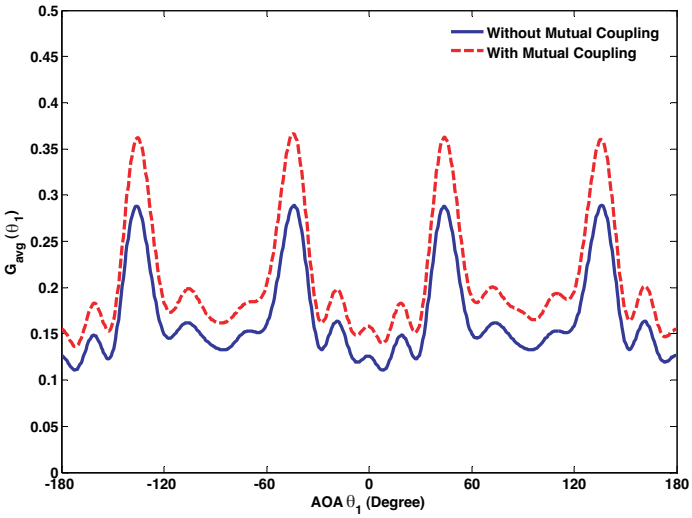

(b)

Figure 10. (a) Geometry of "1 + 3 + 5 elements CCAA"; (b) Variations of $G_{avg}(\theta_1)$ for the "1 + 3 + 4 elements CCAA", with and without MC; with $r_1 = \lambda$, $r_2 = 1.5\lambda$.

$r_2 = 1.5\lambda$, with and without MC is shown in Fig. 10(b). Under no MC assumption, the SIR improvement has an oscillatory variation (see Fig. 10(b)). When MC is included, $G_{avg}(\theta_1)$ of array indicates MC degrades the SIR improvement capability of the array for the most scan angles (see Fig. 10(b)). By comparing the result of this and "3 + 5 elements CCAA", we conclude that the ripple of the $G_{avg}(\theta_1)$ in "1 + 3 + 5 elements CCAA" is noticeable. On the other hand, because

of the flatten curve the array performance of "3 + 5 elements CCAA" (symmetrical geometry), is more consistent than "1 + 3 + 4 elements CCAA" array (has the center element).

5. CONCLUSION

It is very important to search for the best SIR performance based on fixed number of elements. In this paper some configurations of eight and nine elements of CA and CCAA, with and without the element in the center by using circular patch antenna is investigated. Tow cases, one where MC is neglected and a second where MC is include, have been considered. Under MC assumption, the symmetric CCAA without center element (e.g., "4 + 4 elements CCAA") is the beast, because of:

a) Its total average of the spatial interference suppression coefficient is minimum.
b) Its $G_{avg}(\theta_1)$ is the most flatten curve.
c) It has been shown its pattern characteristics is the best.

So, it has the best SIR performance. Finally, we concluded that:

1. In arrays when the total average of spatial interference suppression coefficient is low, then the pattern characteristics is high.
2. In order to keep SIR performance consistent in total range of 360°, the array configuration must be symmetric.
3. In some configurations MC degrades SIR improvement capability, but it can not be consider as a general role.
4. If CCAA has center element, the SIR performance will not be consistent in all scan angles.

REFERENCES

1. Tsoulos, G. V. (ed.), *Adaptive Antennas for Wireless Communications*, IEEE Press, New York, 2001.
2. Rappaport, T. S. (ed.), *Smart Antennas: Adaptive Arrays, Algorithms & Wireless Position Location*, IEEE Press, New York, 1998.
3. Song, Y. S. and H. M. Kwon, "Analysis of a simple smart antenna for CDMA wireless communications," *Proc. IEEE Vehicular Technology Conf.*, 254–258, San Antonio, TX, May 1999.
4. Adve, R. S. and T. K. Sarkar, "Compensation for the effects of mutual coupling on direct data domain adaptive algorithms," *IEEE Trans. Antennas Propagat.*, Vol. 48, 86–94, Jan. 2000.

5. Choi, S. and D. Yun, "Design of adaptive antenna array for tracking the source of maximum power and its application to CDMA mobile communications," *IEEE Trans. Antennas Propagat.*, Vol. 45, 1393–1404, Sept. 1997.
6. Colman, G. W. K. and S. D. Blostein, "Improved power and capacity predictions of a CDMA system with base-station antenna arrays and digital beamforming," *Proc. 19th Biennial Symp. Communications*, 280–284, Kingston, June 1998.
7. Durrani, S. and M. E. Bialkowski, "Investigation into the performance of a adaptive array in cellular environment," *Proc. IEEE AP-S Int. Symp.*, Vol. 2, 648–651, San Antonio, TX, June, 2002.
8. Song, Y. S., H. M. Kwon, and B. J. Min, "Computationally efficient smart antennas for CDMA wireless communications," *IEEE Trans. Veh. Technol.*, Vol. 50, 1613–1628, Nov. 2001.
9. Wyglinski, A. M. and S. D. Blostein, "Mutual coupling and scattering effects on cellular CDMA systems using smart antennas," *Proc. IEEE VTC 2000 Fall*, Vol. 4, 1656–1662, Boston, MA, Sept. 2000.
10. Mahmoud, K. R., M. El-Adawy, S. M. M. Ibrahem, R. Bansal, and S. H. Zainud-Deen, "A comparison between circular and hexagonal array geometries for smart antenna systems using particle swarm optimization algorithm," *Progress In Electromagnetics Research*, PIER 72, 75–90, 2007.
11. Durrani, S. and M. E. Bialkowski, "Effect of mutual coupling on the interference rejection capabilities of linear and circular arrays in CDMA systems," *IEEE Trans. on Antennas and Propagation*, Vol. 52, 1130–1134, 2004.
12. Dessouky, M., H. Sharshar, and Y. Albagory, "Optimum normalized-Gaussian tapering window for side lobe reduction in uniform concentric circular array," *Progress In Electromagnetics Research*, PIER 69, 35–46, 2007.
13. Chen, T. B., Y. L. Dong, Y. C. Jiao, and F. S. Zhang, "Synthesis of circular antenna array using crossed particle swarm optimization algorithm," *J. of Electromagn. Waves and Appl.*, Vol. 20, No. 13, 1785–1795, 2006.
14. Dessouky, M., H. Sharshar, and Y. Albagory, "A novel tapered beamforming window for uniform concentric circular arrays," *J. of Electromagn. Waves and Appl.*, Vol. 20, No. 14, 2077–2089, 2006.
15. Fu, Y. Q., Q. R. Zheng, Q. Gao, and G. H. Zhang, "Mutual coupling reduction between large antenna arrays using

electromagnetic bandgap (EBG) structures," *J. of Electromagn. Waves and Appl.*, Vol. 20, No. 6, 819–825, 2006.

16. Wan, J. X., J. Lei, and C.-H. Liang, "An efficient analysis of large scale periodic microstrip antenna arrays using the characteristic basis function method," *Progress In Electromagnetics Research*, PIER 50, 61–81, 2005.
17. Mouhamadou, M., P. Armand, P. Vaudon, and M. Rammal, "Interference suppression of the linear antenna arrays controlled by phase with use of SQP algorithm," *Progress In Electromagnetics Research*, PIER 59, 251–265, 2006.
18. Sanyal, S. K., Q. M. Alfred, and T. Chakravarty, "A novel beam switching algorithm for programmable phased array antenna," *Progress In Electromagnetics Research*, PIER 60, 187–195, 2006.
19. Dessouky, M., H. Sharshar, and Y. Albagory, "Efficient sidelobe reduction technique for small-sized concentric circular arrays," *Progress In Electromagnetics Research*, PIER 65, 187–200, 2006.
20. IE3D, Zeland Software. IE3D User's Manual Release 9. Zeland Software Inc. [Online] Available: http://www.zeland.com.
21. Grag, R., P. Bhartia, I. Bahal, and A. Ittipiboon, *Microstrip Antenna Design Handbook*, 2nd edition, Artech House, 2001.
22. Choi, S. and D. Yun, "Design of adaptive antenna array for tracking the source of maximum power and its application to CDMA mobile communications" *IEEE Trans. Antennas Propagat.*, Vol. 45, 1393–1404, Sept. 1997.
23. Styeskal, H. and J. S. Herd, "Mutual coupling compensation in small array antennas," *IEEE Trans. AP*, Vol. 38, No. 12, 1971–1975, 1990.
24. Gozasht, F., G. R. Dadashzadeh, and S. Nikmehr, "A comprehensive performance study of circular and hexagonal array geometries in the LMS algorithm for smart antenna applications," *Progress In Electromagnetics Research*, PIER 68, 281–296, 2007.